AGU PUBLICATIONS

JGR

Journal of Geophysical Research: Atmospheres

RESEARCH ARTICLE
10.1002/2016JD025626

Bellingshausen Sea ice extent recorded in an Antarctic Peninsula ice core

Stacy E. Porter[1], Claire L. Parkinson[2], and Ellen Mosley-Thompson[1,3]

[1]Byrd Polar and Climate Research Center, Ohio State University, Columbus, Ohio, USA, [2]Cryospheric Sciences Laboratory, NASA Goddard Space Flight Center, Greenbelt, Maryland, USA, [3]Department of Geography (Atmospheric Sciences Program), Ohio State University, Columbus, Ohio, USA

Key Points:
- Ice core-derived accumulation from Antarctic Peninsula preserves a signal of Bellingshausen Sea ice extent
- Accumulation and sea ice respond similarly to large-scale climate oscillations (e.g., SAM, ENSO, and TPI)
- Recent trends of increased accumulation and decreased Bellingshausen Sea ice extent are unique for the twentieth century

Supporting Information:
- Supporting Information S1

Correspondence to:
S. E. Porter,
porter.573@osu.edu

Citation:
Porter, S. E., C. L. Parkinson, and E. Mosley-Thompson (2016), Bellingshausen Sea ice extent recorded in an Antarctic Peninsula ice core, *J. Geophys. Res. Atmos.*, *121*, 13,886–13,900, doi:10.1002/2016JD025626.

Received 8 JUL 2016
Accepted 12 NOV 2016
Accepted article online 16 NOV 2016
Published online 3 DEC 2016

Abstract Annual net accumulation (A_n) from the Bruce Plateau (BP) ice core retrieved from the Antarctic Peninsula exhibits a notable relationship with sea ice extent (SIE) in the Bellingshausen Sea. Over the satellite era, both BP A_n and Bellingshausen SIE are influenced by large-scale climatic factors such as the Amundsen Sea Low, Southern Annular Mode, and Southern Oscillation. In addition to the direct response of BP A_n to Bellingshausen SIE (e.g., more open water as a moisture source), these large-scale climate phenomena also link the BP and the Bellingshausen Sea indirectly such that they exhibit similar responses (e.g., northerly wind anomalies advect warm, moist air to the Antarctic Peninsula and neighboring Bellingshausen Sea, which reduces SIE and increases A_n). Comparison with a time series of fast ice at South Orkney Islands reveals a relationship between BP A_n and sea ice in the northern Weddell Sea that is relatively consistent over the twentieth century, except when it is modulated by atmospheric wave patterns described by the Trans-Polar Index. The trend of increasing accumulation on the Bruce Plateau since ~1970 agrees with other climate records and reconstructions in the region and suggests that the current rate of sea ice loss in the Bellingshausen Sea is unrivaled in the twentieth century.

1. Introduction

Sea ice plays several extremely important roles in the climate system. Among them, it serves as a barrier between the ocean and the atmosphere, thereby reducing the exchange of heat, mass, and momentum, and it is a crucial component of the ice-albedo feedback system, wherein it greatly impacts the amount of solar radiation absorbed at the surface through its reflection of most of the incident solar radiation [*Parkinson*, 2004]. The formation and decay of sea ice also influence the salinity and density of the ocean, which in turn impact ocean waves and currents. Biologically, oceanic productivity is modulated by the location of the sea ice margin, and many life forms, from the bottom to the top of the polar ecosystem food chain, depend on sea ice as a part of their habitats [*Ainley et al.,* 2003; *Post et al.,* 2013]. Low-level baroclinicity, created by the thermal contrast between sea ice and open water, can also influence the regional tracks of cyclones [*Kvamstø et al.,* 2004].

Arctic sea ice has been rapidly declining in the past several decades, while Antarctic sea ice trends have been lower in magnitude and, overall, in the opposite direction. Since November 1978, when the long-term multichannel passive-microwave satellite record of sea ice began, sea ice around the Antarctic continent has increased by about 5–8%. The positive trend exists for all 12 months, although there are noticeable temporal and regional variations [*Parkinson and Cavalieri*, 2012]. The strongest positive trend comes from changes in the Ross Sea, while the Bellingshausen/Amundsen Seas have experienced a marked decline in sea ice extent [*Parkinson and Cavalieri*, 2012]. This asymmetry in the ice extent trends in the Ross versus Bellingshausen/Amundsen Seas has been attributed at least in part to changes in meridional winds associated with sea level pressure (SLP) anomalies in the Amundsen Sea region [*Lefebvre et al.,* 2004; *Stammerjohn et al.,* 2008; *Holland and Kwok*, 2012].

The Amundsen Sea Low (ASL) is a climatological low-pressure system induced by the unique orography of Antarctica [*Baines and Fraedrich*, 1989; *Lachlan-Cope et al.,* 2001] and roughly defines the location of the climatological storm track [*Fogt et al.,* 2012]. Variability in the ASL has a large influence on the climate of the Antarctic Peninsula (AP) by substantially controlling cyclone strength and frequency as well as warm air advection from the north [*Turner et al.,* 2013; *Raphael et al.,* 2016]. *Fogt and Wovrosh* [2015] found recent deepening trends in the ASL that are explained primarily by tropical sea surface temperatures

and radiative forcing. The deepening of the ASL coincides with intense warming on the AP [*Turner et al.,* 2005] and the collapse of ice shelves along the peninsula [*Scambos et al.,* 2004]. Projections of the ASL anticipate a further deepening [*Zheng et al.,* 2013; *Hosking et al.,* 2016] and a poleward shift [*Hosking et al.,* 2016] accompanied by a positive trend in the Southern Annular Mode (SAM) [*Shindell and Schmidt*, 2004].

The strength of the ASL depends on several factors, including large-scale climatic oscillations like SAM and tropical forcing from the El Niño–Southern Oscillation (ENSO) [*Kwok and Comiso*, 2002; *Lachlan-Cope and Connolley*, 2006; *Fogt et al.,* 2012; *Clem and Fogt*, 2013; *Turner et al.,* 2013]. SAM, defined as the pressure gradient between the southern middle and high latitudes, is a primary control on Antarctic climate [*Gong and Wang*, 1999; *Thompson and Wallace*, 2000]. A positive phase of SAM is associated with lower-pressure anomalies over the Antarctic continent, stronger circumpolar westerlies, and a deepening ASL. A negative SAM is the reversal of this pattern, with higher-pressure anomalies over the continent, weaker westerlies, and a weaker ASL. In recent decades, the overall trend for the SAM has been positive [*Thompson and Solomon*, 2002; *Marshall*, 2003; *Thompson et al.,* 2011], and modeling studies project this trend to continue through the 21st century under enhanced greenhouse gas forcing [*Fyfe et al.,* 1999; *Kushner et al.,* 2001; *Cai et al.,* 2003; *Shindell and Schmidt*, 2004].

The El Niño concept originated from variations in tropical Pacific Ocean temperatures, but considerable work during the twentieth century established that these regional ocean temperature variations are tied closely to regional atmospheric pressure variations (i.e., Southern Oscillation) and to climate variations over much larger areas. Now it is recognized that ENSO entails far-reaching effects around the globe, including Antarctica [*Turner*, 2004; *Fogt and Bromwich*, 2006; *Stammerjohn et al.,* 2008; *Clem and Fogt*, 2013, 2015]. During La Niña events (the cold counterpart to the warm central and eastern tropical Pacific during El Niño events), the South Pacific Convergence Zone (SPCZ) shifts southwestward, establishing a connection between the tropical Pacific and southern high latitudes [*Vincent*, 1994; *Chen et al.,* 1996], in particular, the AP [*Clem and Fogt*, 2015; *Goodwin et al.,* 2016]. During El Niño events, the SPCZ shifts northward toward the equator, and tropical convection is directed toward South America [*Eichler and Gottschalck*, 2013].

The coupling of SAM and ENSO modulates the response to these phenomena in the high latitudes, as it can amplify or dampen their respective impacts. Their in-phase coupling (e.g., positive SAM/La Niña and negative SAM/El Niño) tends to amplify their influence on the Antarctic [*Gong et al.,* 2010, 2013; *Fogt et al.,* 2011; *Ding et al.,* 2012]. When out-of-phase (e.g., positive SAM/El Niño and negative SAM/La Niña), SAM appears to modulate the tropical influence over the high-latitude climate, but there are many uncertainties, and these SAM and ENSO interactions remain an area of active research [*Fogt and Bromwich*, 2006; *L'Heureux and Thompson*, 2006; *Fogt et al.,* 2011; *Clem and Fogt*, 2013; *Goodwin et al.,* 2016]. Nevertheless, the combination of the SAM and ENSO, and their associated impacts on the ASL and storm tracks, influences temperature and precipitation near the AP, thereby ultimately affecting both sea ice in that region and accumulation on the Bruce Plateau (Figure 1).

Several recent studies indicate that the SAM's influence on the climate of Antarctica is nonstationary [*Silvestri and Vera*, 2009; *Marshall et al.,* 2013; *Goodwin et al.,* 2016]. Their results suggest limitations on the ability to reconstruct variability in the climate system based on short calibration periods. The most reliable and complete records of sea ice extent are available from satellites dating back to the 1970s, although their short duration inhibits the examination of multidecadal variability and the stationarity of recently discerned relationships. To explore the dynamics between large-scale teleconnections and sea ice extent, longer records are necessary. With that in mind, an ice core from the AP is investigated to determine how well it captures regional sea ice extent and the feasibility of using ice core-derived sea ice reconstructions to elucidate the changing influences of large-scale circulation patterns.

Local sea ice reconstructions have been generated previously using ice cores from around the Antarctic continent. Given their marine source, methanesulphonic acid (MSA) and sea salt components are primarily used in these reconstructions [*Abram et al.,* 2013]. Results suggest that sea salt and sea ice extent are related on glacial/interglacial time scales [*Wolff et al.,* 2006; *Röthlisberger et al.,* 2010] but less so interannually [*Abram et al.,* 2013] and that MSA can serve as a reasonable proxy for interannual sea ice variability, especially for coastal sites where transport processes do not dominate [*Abram et al.,* 2013].

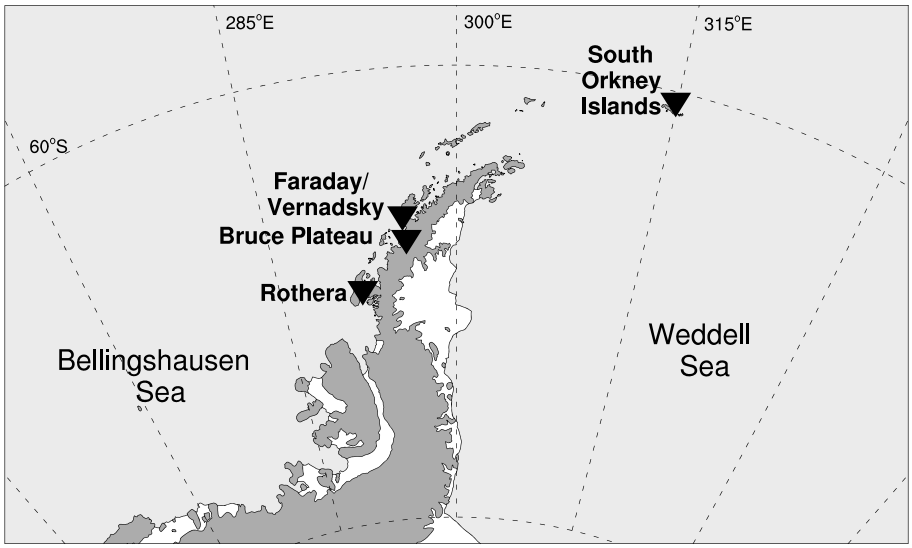

Figure 1. Map of the Antarctic Peninsula region.

Curran et al. [2003] used the MSA record from the Law Dome ice core from coastal East Antarctica to suggest a decline in regional sea ice extent (for the 80°–140°E sector) since the 1950s. However, the relationship between MSA and sea ice extent varies greatly depending on the region of Antarctica studied [*Abram et al.,* 2007, 2013]. For example, in the Weddell Sea, the offshore southerly winds associated with (and perhaps causing) extensive sea ice reduce the transport of MSA to core sites along the southern coast [*Abram et al.,* 2007]. In contrast, in the Bellingshausen Sea, enhanced sea ice extent, and subsequent algae blooms along the margins, leads to increased MSA in three cores (i.e., James Ross Island, Dyer Plateau, and Beethoven Peninsula) along the AP [*Abram et al.,* 2010].

Dixon et al. [2005] divided sulfate records from the International Trans-Antarctic Scientific Expedition (ITASE) cores in West Antarctica into sea salt and excess/biogenic sulfate components. They found higher sea salt sulfate associated with more extensive sea ice, which they linked to the development of frost flowers. On the other hand, the excess/biogenic sulfate component was associated with reduced sea ice extent in the Amundsen/Bellingshausen Sea region, since sea ice cover can inhibit dimethylsulfide emissions from biological activity.

Küttel et al. [2012] found that the relationship between stable water isotopes ($\delta^{18}O$ and δD) in a suite of ITASE cores from West Antarctica and sea ice in the Amundsen Sea was linked to the influence of the ASL on meridional flow. Similarly, *Thomas et al.* [2013] determined that hydrogen isotopes (δD) from the West Antarctic Ferrigno ice core are related to the maximum sea ice extent in the Amundsen/Bellingshausen Sea region due to the influence of meridional winds.

In this study, an ice core from the western AP is tested for its potential to reconstruct sea ice conditions off the western coast of the AP. We show that for this particular ice core, accumulation, rather than the other variables used in the aforementioned studies, is most strongly related to sea ice extent in the Bellingshausen Sea. Although sea ice extent can directly influence precipitation via moisture source availability, it is also probable that large-scale climate patterns are the primary drivers of both sea ice extent and accumulation. Hence, despite the nonstationary responses to these large-scale drivers over multidecadal time scales, the sea ice extent and land-based snow accumulation are expected to exhibit a consistent pattern of changes.

2. Data

The 448.12 m Bruce Plateau (BP) ice core was drilled to bedrock in 2010 from the Antarctic Peninsula (66.03°S; 64.07°W; 1975.5 m above sea level). The site experiences virtually no melting, and only three very thin (<3 mm) melt layers were observed in the entire core. Borehole temperatures reveal that the average temperature for the most recent year is −14.78°C (measured at 15 m), the minimum temperature of −15.8°C

occurs at 173 m, and the ice is frozen to the bed with a basal temperature estimated to be −10.2°C [*Zagorodnov et al.,* 2012].

The core was cut into discrete samples and concentrations of MSA, and other ionic species were measured by ion chromatography (Dionex ICS-3000) in a Class 100 Clean Room. Seasonally varying concentrations of MSA due to biogenic activity [*Curran and Jones*, 2000; *Curran et al.,* 2003], complemented by gross beta radioactivity [*Pourchet et al.*, 1983] (Figure S1 in the supporting information), allow for a precise annual time scale with an uncertainty of less than one year from 1900 to 2009 [*Goodwin et al.,* 2016]. Annual delineations are marked by summer MSA maxima that may vary slightly in timing during the summer months such that each annual layer roughly corresponds to a calendar year. This slight timing uncertainty, along with postdepositional effects such as compaction, wind scouring, erosion, and evaporation/sublimation, could introduce modest errors when reconstructing the annual net accumulation (A_n). In addition, MSA has been shown in some instances to migrate with depth such that MSA deposited in summer eventually migrates to the winter layer below [*Pasteur and Mulvaney*, 2000; *Thomas and Abram*, 2016]. The first evidence of very modest MSA migration in the BP core occurs at ~380 m representing snow deposited in ~1567 Common Era, well below the reference period for this study. MSA migration is clearly evident at 395 m (Figure S2 in the supporting information).

The BP site experiences a remarkably high rate of accumulation (annual average from 1900 to 2009 is 1.84 m water equivalent), which greatly minimizes dating errors resulting from postdepositional effects. To account for thinning and compaction, the *Dansgaard and Johnsen* [1969] model, a modified version of the *Nye* [1963] model, was used to reconstruct the original thicknesses of the annual layers using a strain rate transition depth estimated by *MacGregor et al.* [2012] (see further discussion in the supporting information). The high accumulation rate is in large part explained by the fact that the west coast of the AP is frequently inundated with maritime air flow from the Bellingshausen Sea. Thus, the sea ice extent in the Bellingshausen Sea should produce some signal in the BP ice core, as it provides a major control over the primary moisture source.

Sea ice extents in the Bellingshausen Sea were determined from satellite passive-microwave data from the scanning multichannel microwave radiometer (SMMR) on NASA's Nimbus 7 satellite and the Special Sensor Microwave Imager (SSMI) and SSMI/Sounder (SSMIS) on satellites of the Department of Defense's Defense Meteorological Satellite Program. The SMMR instrument was launched in late October 1978 and provided a record of sea ice observations until mid-August 1987. The first SSMI was launched in June 1987, and the series of SSMI/SSMIS measurements continues. Microwave observations allow the determination of the distribution and extent of the sea ice cover year-round, irrespective of day versus night conditions and largely irrespective of cloud-free versus cloudy conditions. SMMR provided an every-other-day record, and the SSMI and SSMIS instruments have provided a daily record since mid-1987. The SMMR, SSMI, and SSMIS data are mapped onto approximately 25 km × 25 km grid cells. For each ocean grid cell, the ice concentration, defined as the percent areal coverage of sea ice in the grid cell, is calculated. Ice extent is then calculated as the sum of the areas of all grid cells (in the region of interest, in this case the Bellingshausen Sea) with a calculated ice concentration of at least 15% [*Parkinson and Cavalieri*, 2012]. For these calculations, we used the Antarctic Peninsula and, north of the Peninsula, longitude 60°W as the eastern boundary of the Bellingshausen Sea, latitude 55°S as the northern boundary, longitude 99°W as the western boundary, and the Antarctic continent as the southern boundary.

The Amundsen Sea Low (ASL) characteristics were obtained from the European Centre for Medium-Range Weather Forecasts Interim Reanalysis (ERA-Interim) for the region bounded by latitudes 60 and 80°S and longitudes 170 and 298°E [*Hosking et al.,* 2016]. These data include the average SLP over the entire sector, the central pressure of the ASL, and the location (latitude and longitude) of the lowest central pressure. The annual SAM index (1957–2009) is calculated from monthly SAM values of the SLP gradient between the middle and high latitudes using station pressure observations [*Marshall*, 2003]. The Southern Oscillation Index (SOI), the atmospheric component of the ENSO, is calculated as the difference in SLP between Tahiti and Darwin [*Ropelewski and Jones*, 1987; *Allan et al.,* 1991; *Können et al.,* 1998]. The Trans-Polar Index (TPI) [*Pittock*, 1980, 1984; *Jones et al.,* 1999] is calculated from the normalized pressure difference between Hobart, Australia (43°S; 147°E) and Stanley, Falkland Islands (52°S; 58°W) and highlights oscillations in the troughing and/or ridging between New Zealand and South America known as wave number 1. The TPI data were detrended to account for external forcing such as the increasing SAM trend due to stratospheric ozone loss and increased greenhouse gases. Gridded meteorological data were acquired from the National

Center for Environmental Prediction/National Center for Atmospheric Research reanalysis for 1979–2012, updated from *Kalnay et al.* [1996].

The duration and dates of formation and breakout of sea ice in the northwest Weddell Sea from 1903 to 2008 were obtained from an observational sea ice record from the South Orkney fast-ice (SOFI) series [*Murphy et al.,* 1995, 2014], providing a far longer record than is possible with the satellite data alone. The South Orkney observations were manual until 1994 and have been maintained thereafter with an automatic camera system [*Murphy et al.,* 2014].

3. Results

Correlations between annual Bellingshausen Sea sea ice extent (Bellingshausen SIE) and the annual data for several variables from the BP ice core, including A_n, stable water isotopes, and major anion and cation fluxes, are computed for the period 1979–2009. All correlations account for autocorrelation using random phase testing described by *Ebisuzaki* [1997]. Significant (>95%) negative correlations are obtained for several of the variables, including sea salt components (Na^+, Cl^-, and SO_4^{2-}; $r \approx -0.46$ for each variable) and isotopes ($\delta^{18}O$ and δD; $r \approx -0.55$ for both variables). Surprisingly, MSA is only weakly correlated ($r = 0.21$; $p = 0.271$) to Bellingshausen SIE on the annual time scale. One possibility for the low correlation is that a portion of the MSA reaching Bruce Plateau may originate from other marine sources, such as the Weddell Sea or the Drake Passage between the peninsula and South America. The MSA precursor, dimethylsulfide, originates from biological activity within the sea ice margin and is also subject to transport and oxidation processes that influence its deposition over the drill site [*Thomas and Abram*, 2016]. The strongest correlation is between Bellingshausen SIE and A_n ($r = -0.67$; $p < 0.001$; Figure 2). Over the satellite era, both Bellingshausen SIE and BP A_n show significant (>99%) decreasing and increasing trends, respectively. These trends explain ~25% of the variance; however, the correlation coefficient between the detrended variables is still highly significant ($r = -0.56$; $p = 0.005$).

Correlations between annual BP A_n and seasonal Bellingshausen SIE (Table 1) are strongest in autumn (April-May-June (AMJ): $r = -0.695$; $p < 0.001$) and winter (July-August-September (JAS): $r = -0.58$; $p = 0.002$), when sea ice is growing and at maximum extent, respectively. Correlations between the BP annual fluxes of anions and cations and seasonal Bellingshausen SIE are also strongest in austral autumn and winter, which is not unexpected as these anions and cations are deposited primarily by wet deposition and the flux calculation is dependent on accumulation. Thus, the moderate correlations among the BP chemical species and Bellingshausen SIE are considered to be primarily artifacts of their covariability with accumulation. Linear regression was used to model the relationships between BP A_n and various constituents and to remove the influence of A_n on the anions and cations, and the subsequent residuals were correlated with Bellingshausen SIE. For all the residual variables from which A_n has been linearly removed, the significance of correlations with Bellingshausen SIE falls well below the 95% confidence level.

Although SIE and accumulation can be directly related through the availability of moisture from open water, it is hypothesized here that the sea ice extent and accumulation also have a shared response to larger-scale climate drivers. This inference applies to the broad-scale picture, not to individual events; for example, the large 1997/1998 El Niño event was associated with greatly reduced BP A_n in 1997 but had much less effect on Bellingshausen SIE (Figure 2).

To investigate some of the large-scale climatic influences on Bellingshausen SIE and BP A_n, composites of sea level pressure (SLP) were generated to determine the SLP difference between the 5 years with the most extensive and the 5 years with the least extensive sea ice coverage and between the five lowest and five highest A_n years (Figure 3). Given the strong correlation between Bellingshausen SIE and BP A_n, the composites share similar years and seasons when SIE is high and A_n is low, and vice versa. These SLP composites reveal a discernibly strong influence of the ASL on both SIE and A_n. As expected, higher SLP in the Amundsen/Bellingshausen Sea region, and hence a weaker ASL, is associated with enhanced sea ice extent and reduced BP A_n. A stronger ASL, and its accompanying cyclonic flow, would advect warm, moist air from the north toward the AP thereby reducing sea ice extent and increasing BP A_n.

Hosking et al. [2016] generated several ASL variables from ERA-Interim including ASL sector pressure, ASL central pressure, and the longitude and latitude of the central pressure. Central pressure of the ASL and

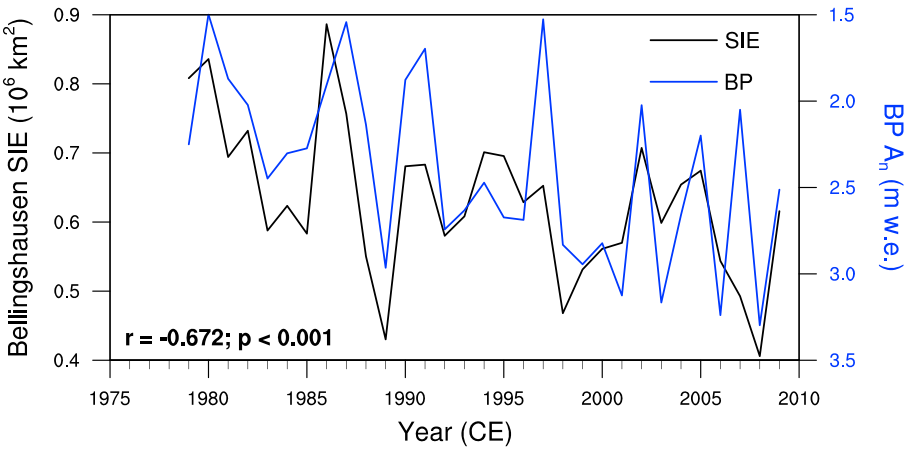

Figure 2. Time series of Bellingshausen SIE (black) and BP A_n (blue; axis inverted).

average pressure over the ASL sector (60–80°S; 170–298°E) are inherently related, but Bellingshausen SIE responds most strongly to the sector-wide SLP. The relationship between the ASL sector pressure and the Bellingshausen SIE (Figure 4) is strongest on the annual time scale ($r = 0.646$; $p < 0.001$). Seasonally, the relationship is strongest in autumn (AMJ) and winter (JAS) ($r = 0.488$; $p = 0.03$ for both seasons) and weakest in summer (January-February-March (JFM): $r = 0.340$; $p = 0.126$). The ASL sector pressure has a similar influence on BP A_n (Table 1), with the strongest relationship on the annual scale ($r = -0.58$; $p = 0.003$). The correlations between seasonal ASL sector pressures and annual BP A_n (Table 1) are highest for autumn (AMJ: $r = -0.48$; $p = 0.006$) and spring (October-November-December (OND): $r = -0.41$; $p = 0.014$), which are the transitional time periods for sea ice extent. No significant correlations were observed between the location of the ASL and either BP A_n or Bellingshausen SIE, suggesting that the climate of this region is more heavily influenced by the depth of the ASL than by its exact position.

The depth of the ASL depends on numerous factors, including large-scale climatic oscillations like SAM and ENSO [*Kwok and Comiso*, 2002; *Fogt et al.,* 2012; *Clem and Fogt*, 2013; *Turner et al.,* 2013]. The SLP composites in Figure 3 reflect not only the influence of the ASL on AP climate but also the pressure differences between the high and midlatitudes, a signature of SAM. Figure 5 reveals the statistically significant negative relationships between Bellingshausen SIE and both SAM (Figure 5a) and SOI (Figure 5b). A positive SAM and positive SOI (La Niña event) serve to deepen the ASL, which increases the advection of warm, moist air from the north to the Bellingshausen Sea and the AP. This warm, moist air advection tends to decrease sea ice extent and increase accumulation at the BP site. On the annual time scale, the relationship of Bellingshausen SIE with SOI is slightly stronger than that with SAM (Figure 5). The two lowest ice extent years (1989 and 2008) coincide with strong La Niña events. *Fogt and Bromwich* [2006] noted decadal variability in the response of geopotential height fields over the Amundsen/Bellingshausen Seas to both SAM and SOI, specifically a stronger response in the 1990s versus the 1980s. *Clem and Fogt* [2013] argue that the weaker response in the 1980s is a statistical artifact of the strong 1988/89 La Niña event, the effects of which were dampened by a concurrent negative SAM. However, *Clem and Fogt* [2013] focused primarily on austral spring. In this study, where BP A_n is constrained to annual resolution, we find the following annually averaged conditions during the 1988/1989 La Niña event: very low Bellingshausen SIE, high 1989 BP A_n, a positive SOI, a negative 1988 SAM, and a positive 1989 SAM (Figures 2 and 5).

Table 1. Correlation Coefficients Between Annual BP A_n and Annual and Seasonal Antarctic Climate Variables[a]

BP A_n	ANN	JFM	AMJ	JAS	OND
Bellingshausen SIE	**−0.67***	**−0.42**	**−0.69***	**−0.58***	**−0.37**
ASL sector pressure	**−0.58***	−0.21	**−0.48***	−0.31	**−0.41**
SAM	**0.57***	0.23	**0.37**	0.21	**0.42**
SOI	**0.45**	0.24	0.35	0.34	**0.38**

[a]Bold and asterisks indicate 95% and 99% significance levels, respectively. ANN = Annual; JFM = January-February-March; AMJ = April-May-June; JAS = July-August-September; and OND = October-November-December.

Goodwin et al. [2016] provide extensive detail on the relationships

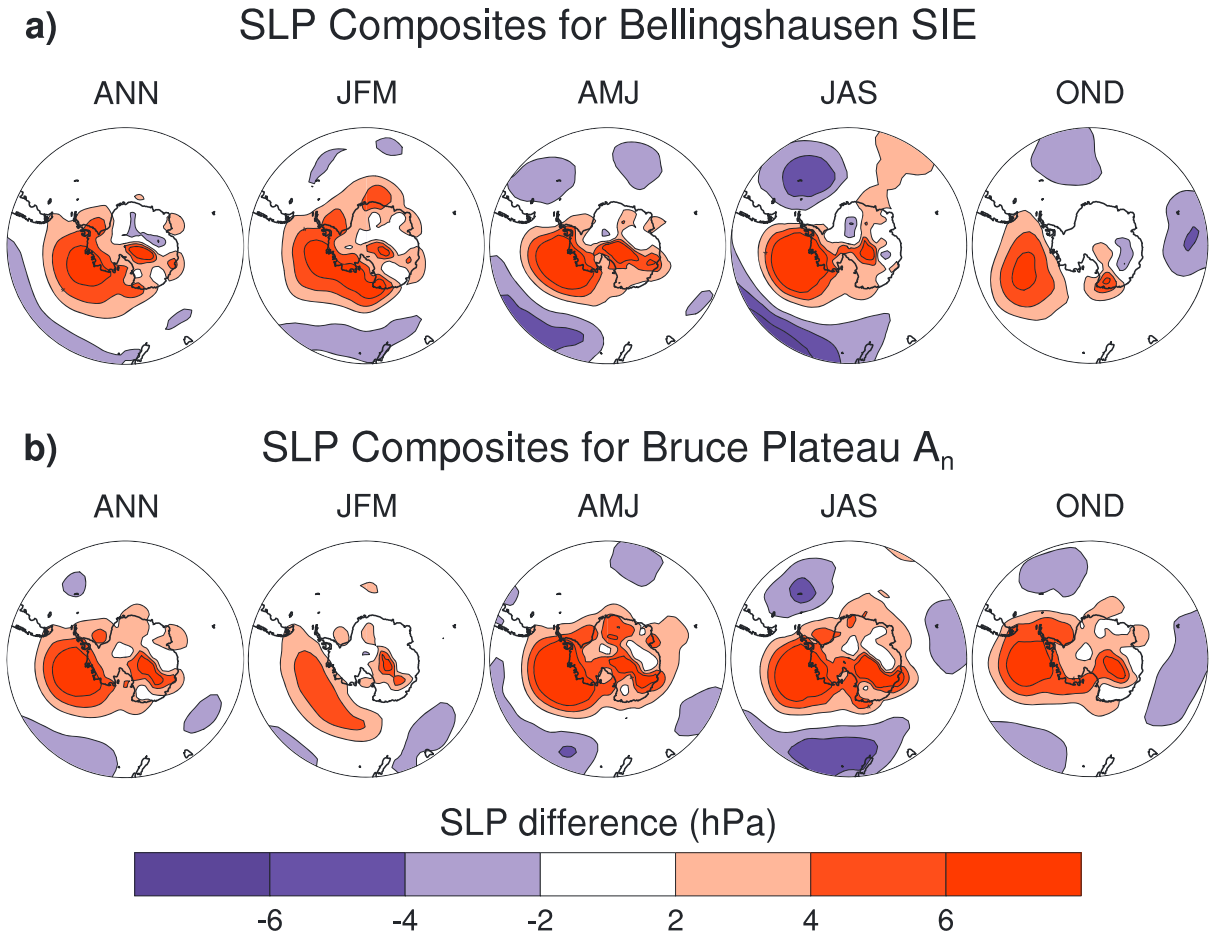

Figure 3. Composites showing the annual and seasonal SLP (hPa) differences between (a) the five most extensive and the five least extensive SIE years or seasons in the Bellingshausen Sea and (b) the five lowest and five highest BP A_n years. Numbers of shared years (out of 10) among SIE and A_n composites are as follows: ANN (4), JFM (5), AMJ (6), JAS (5), and OND (2).

between BP A_n and both SAM and SOI. They determined that the strong positive correlation between SAM and BP A_n observed during the satellite era (Table 1) is only robust since the mid-1970s, prior to which the relationship is negative. They attribute this shift to multidecadal climate variability stemming from the

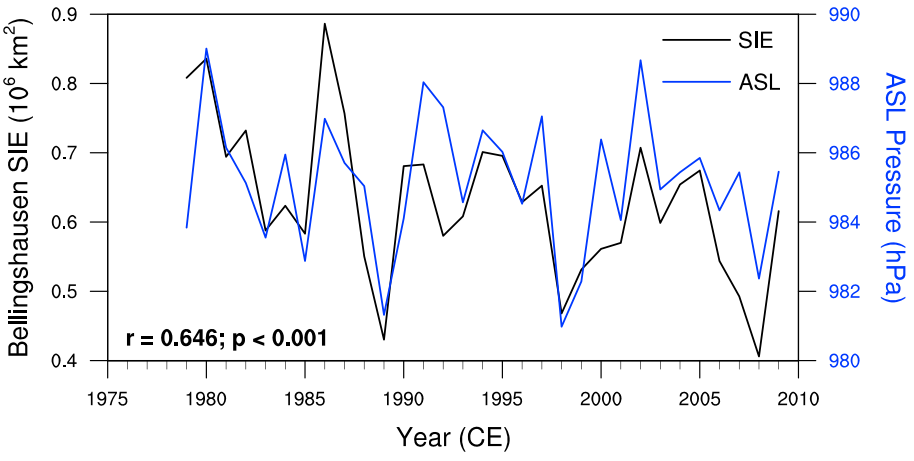

Figure 4. Time series of ASL sector-wide sea level pressure (blue) and Bellingshausen Sea SIE (black), both presented as annual averages.

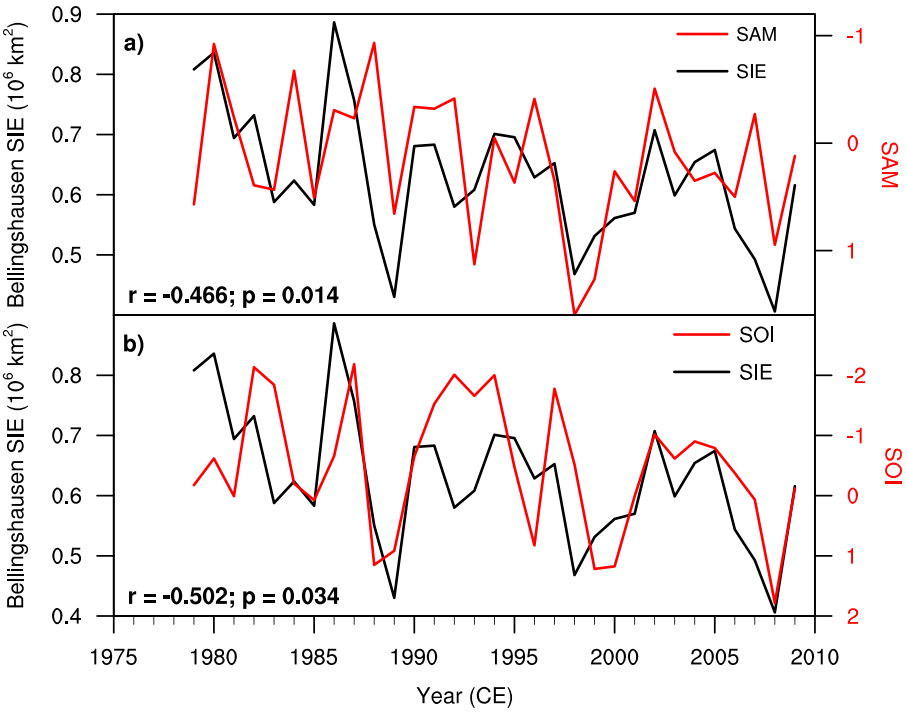

Figure 5. Time series of annual Bellingshausen SIE (black) with (a) SAM (red) and (b) SOI (red). The SAM and SOI axes are inverted.

tropical Pacific. The interactions between SAM and SOI confirm the need for caution when attempting longer-term reconstructions with relatively short calibration periods. Thus, to determine whether the relationship between BP A_n and Bellingshausen SIE is robust, longer records of sea ice are needed for calibration. Fortunately, the fast ice observations from the South Orkney Islands (SOFI) provide continuous dates of sea ice formation and breakout, and hence duration, for most of the twentieth century and into the 21st century (1903–2008) [*Murphy et al.,* 1995, 2014]. The South Orkney Islands are located in the northern Weddell Sea (Figure 1), to the northeast of the Antarctic Peninsula. It is uncertain a priori whether the SOFI series is related to either the Bellingshausen SIE or the BP A_n; however, the timing of SOFI is related to sea ice concentration over much of the northern Weddell Sea and is related to atmospheric circulation west of the Antarctic Peninsula [*Murphy et al.,* 2014].

Regression analysis of BP A_n onto surface zonal winds suggests that both the BP and SOFI sites are influenced by the circumpolar westerlies (Figure 6a). The influence of the zonal winds on BP A_n resembles SAM. *Murphy et al.* [2014] similarly found that the influence of both spring (September-October-November) zonal wind and SLP fields on SOFI breakout date also resembles SAM. Sea surface temperatures (SSTs) in both the Bellingshausen Sea and northwestern Weddell Sea are positively correlated with BP A_n (Figure 6b), suggesting that these regions behave similarly when large-scale forcing influences BP A_n. Despite their geographical differences, the relationships discussed above strongly support the existence of a connection between BP A_n and the SOFI series, likely because both are modulated by similar large-scale forcings.

BP A_n is slightly more strongly correlated with the duration of the sea ice season at South Orkney than with the formation and breakout dates, although the magnitudes of the three correlations are similar and statistically significant (>99%; Figure 7). The slightly higher correlation with the duration likely stems from the fact that the duration is more representative of an annual signal, whereas the timings of formation and breakout are more dependent on autumn and spring, respectively. The correlations between BP A_n and breakout date and duration are negative, indicating that greater accumulation is associated with an earlier breakout date and a shorter sea ice season. The annually contemporaneous formation date and BP A_n were not significantly correlated. However, there is a significant positive correlation when BP A_n leads by 1 year (Figure 7), suggesting that the autumn formation date is partially affected by the conditions of the previous year (e.g., higher

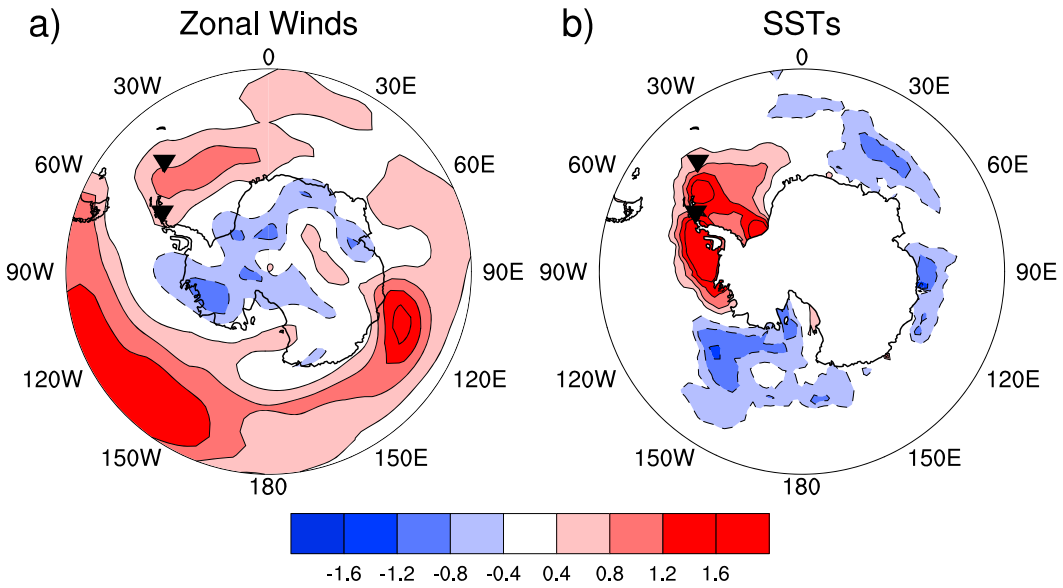

Figure 6. Regression of BP A_n on annual (a) 1000 hPa zonal winds and (b) SSTs for 1979–2009. BP and South Orkney sites are indicated (inverted triangles).

(lower) A_n on the BP site is followed by a(n) later (earlier) SOFI formation date). This is supported by evidence from *Murphy et al.* [2014] suggesting that SOFI formation is related to some preconditioning of SSTs. Furthermore, with regard to SLP patterns, SOFI breakout date appears to be influenced by the SAM, while

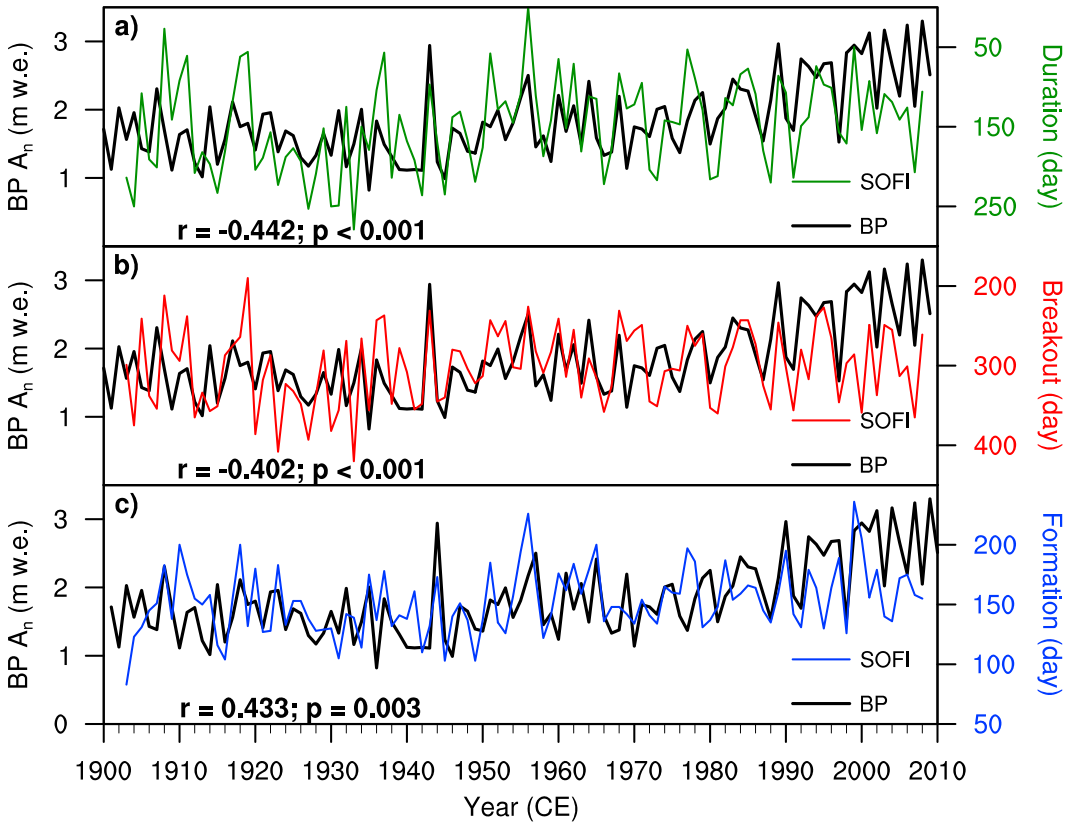

Figure 7. Time series of BP A_n (black) with (a) SOFI duration (green) for the same year, (b) SOFI breakout (red) for the same year, and (c) SOFI formation (blue) for the following year. Duration and breakout axes are inverted.

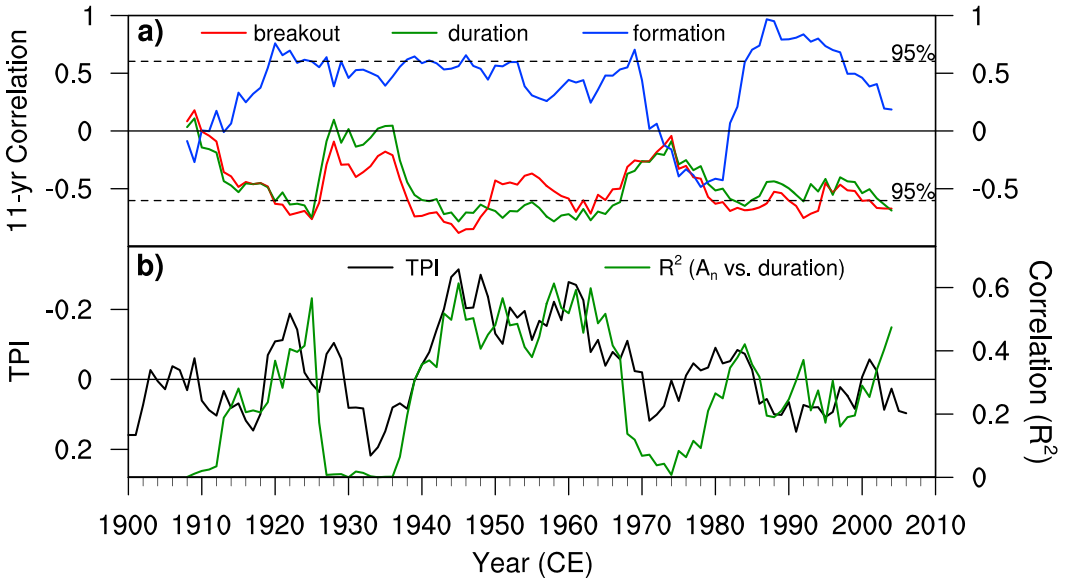

Figure 8. (a) Eleven year running correlations between BP A_n and SOFI breakout (red), duration (green), and formation (lag 1 year; blue). Dashed line represents 95% significance ($r = \pm 0.603$) determined using a two-tailed t test for simplicity. (b) Eleven year running means of the detrended TPI (black; axis inverted) and the strength (R^2) of the relationship between BP A_n and SOFI duration (green).

the formation date appears more strongly connected to SLP anomalies in the South Atlantic [*Murphy et al.,* 2014].

The relationships between BP A_n and the three SOFI time series are statistically significant over the twentieth century (Figure 7), but more importantly, the relationships are relatively robust in that the sign of the correlations is fairly persistent through much of the period (Figure 8a). For the BP site, running correlations reveal that SOFI formation and BP A_n are positively correlated for most of the twentieth century, with the exception of the 1970s. The sign of the relationships between A_n and both SOFI breakout and duration is negative through almost the entire period, although the magnitude varies and is especially low in the 10 years surrounding 1930 and during the 1970s (Figure 8a).

During the 1970s, SAM was predominantly in a negative phase, which results in a weakening of the circumpolar westerlies. As the westerlies likely establish the connection between the western AP and the northwestern Weddell Sea, the negative SAM in the 1970s may explain the weakening of the relationship between BP A_n and both SOFI breakout and duration. However, little agreement exists among SAM reconstructions prior to the midtwentieth century and especially in the 1930s [*Abram et al.,* 2014; *Goodwin et al.,* 2016]. *Abram et al.* [2014] explore some of the differences in the development of these SAM reconstructions, such as detrending and the location of stations or proxies utilized. *Goodwin et al.* [2016] discuss how two SAM reconstructions by *Fogt et al.* [2009] and *Abram et al.* [2014] relate to the TPI over the twentieth century and reflect the circumpolar and regional nature of SAM, respectively. In this study, we find a strong correlation between the TPI and the correlation between BP A_n and SOFI duration (Figure 8b; $r = -0.679$; $p < 0.001$). When the TPI is positive, as during the 1930s and early 1970s, the correlation between BP A_n and SOFI duration weakens considerably (Figure 8b). As the TPI measures the pressure difference between Hobart, Australia, and Stanley, Falkland Islands, a positive value could reflect high pressure at Hobart and/or low pressure at Stanley. The positive TPI in the 1930s resulted from anomalous pressure at both sites, while in the 1970s the positive TPI was primarily due to anomalously low pressure at Stanley [*Pittock*, 1980, 1984; *Jones et al.,* 1999]. Lower pressure over the Falkland Islands suggests more northerly to northeasterly flow over the South Orkney Islands to their southeast, opposing or weakening the typical westerly flow. Northerly flow over this region shortens the SOFI duration, while weaker westerly flow would affect the AP as well, likely reducing BP A_n. With SOFI duration and BP A_n both decreasing, this would weaken or eliminate the negative relationship that exists between BP A_n and SOFI duration during much of the study period (Figure 7). During the brief excursions in the 1930s

and 1970s when the connection between BP A_n and SOFI is weakened under positive TPI conditions, BP A_n is likely more reflective of local sources rather than the regional sources that dominate under positive SAM conditions and the associated strong westerly flow.

With the exception of the weaker relationships observed in the 1930s and 1970s, the running correlations between BP A_n and the SOFI duration are relatively consistent ($r \sim -0.5$) through much of the twentieth century (Figure 8a). Ice core-derived MSA records from around the Weddell Sea, and their subsequent sea ice reconstructions, are not continuously related to the SOFI series and exhibit a sustained, multidecadal shift in the sign of their relationship from ~1945 to ~1975 [*Abram et al.,* 2007]. As mentioned previously, BP A_n exhibits a similar multidecadal shift in the sign of its relationship with SAM. The relationship between BP A_n and SAM is positive for the recent few decades back to the mid-1970s when the relationship abruptly becomes negative. Prior to the mid-1940s, the relationship is again positive [*Goodwin et al.,* 2016]. The SOFI breakout dates show a similar reversal in the sign of its relationship with SAM over the same general time period [*Murphy et al.,* 2014]. Thus, despite the temporally varying influence of SAM at these sites, the accumulation and sea ice exhibit similar responses. This suggests the potential for BP A_n to provide a reasonably realistic reconstruction of annual sea ice extent for the Bellingshausen Sea, since the intricacies and complex interactions among large-scale climate oscillations will similarly influence both the accumulation and sea ice records.

Recent trends in accumulation across Antarctica derived from remote sensing, atmospheric modeling, and ice core-derived reconstructions vary markedly from region to region [*Thomas et al.,* 2015]. An exception is in the Antarctic Peninsula where accumulation has been increasing over the twentieth century with a marked increase in the 1970s, particularly along the west coast as recorded in the BP core and the Gomez core [*Thomas et al.*, 2008]. The trend is less discernible in the 1988 James Ross Island core on the northeastern tip of the peninsula [*Miles et al.*, 2008] and is indiscernible in the centrally located Dyer Plateau core that only extends to 1990 [*Thompson et al.*, 1994] (Figure S3, in the supporting information). Over the first 40 years of the twentieth century, BP A_n was relatively stable, followed by a period of increased variability and then by a prominent upward trend after 1969 (Figure 7). BP A_n is negatively correlated to SOFI duration, which has decreased overall during the twentieth century due to later formation and earlier breakout (Figure 7) [*Murphy et al.,* 2014]. Other ice core-derived sea ice proxies show similar patterns to BP A_n [*Abram et al.,* 2010; *Thomas et al.,* 2013; *Thomas and Abram*, 2016]. MSA records from three cores along the AP reveal a decreasing trend after the midcentury that coincides with reduced winter Bellingshausen SIE [*Abram et al.,* 2010]. On the opposing side of the Antarctic dipole, sea ice extent has been increasing over the Ross Sea, and MSA records from the Ferrigno ice core in West Antarctica reveal that the most recent (mid-1990s) increasing trend is unique for the past few centuries [*Thomas and Abram*, 2016]. Deuterium in the Ferrigno ice core shows an increasing trend in the twentieth century that reflects the observed temperature increase over the AP region as well as the reduction in September sea ice concentration [*Thomas et al.,* 2013], although the authors ultimately found that these trends were not unprecedented in the context of their longer record [*Thomas et al.,* 2013]. Nevertheless, the four highest years of accumulation on the BP occur since 2000, and steep trends, similar to those after 1950, do not occur earlier in the record [*Goodwin*, 2013]. This suggests that the current rate of sea ice loss in the Bellingshausen Sea is unique for the post-1900 period.

4. Discussion and Conclusions

Contemporary climate changes are well documented, and there is concern that the rates of change in the coming decades and centuries may exceed the rate at which humans will be able to adapt comfortably. The complexity of the climate system arises from many natural physical, chemical, and biological connections among the atmosphere, oceans, ice, and land, and the climate system is now also subject to a variety of anthropogenic forcings. Our most geographically complete picture of the detailed interactions within Earth's climate system is now derived from satellite-borne sensors, but such records extend back three to five decades at best. Prediction of future changes requires understanding the preanthropogenic nature of these complex interactions upon which modern forcings are superimposed. Proxy records preserved in many different natural recording systems offer the potential for unique insights to Earth's complex climate system although correctly interpreting these proxy records is often challenging.

Ice cores provide extremely valuable information of different temporal extent and resolution, but such records are geographically sparse and present a range of problems in dating and interpreting the data. The goal of this paper is to determine whether the Bruce Plateau ice core record can facilitate an extension of the satellite-derived record of SIE for the Bellingshausen Sea. Given the natural complexity of the climate system, it is not surprising that a perfect predictor with a one-to-one correspondence to SIE was not identified; however, some interesting and statistically significant relationships do emerge.

Sea ice extent in the Bellingshausen Sea is found to be related to BP A_n ($r = -0.672$; $p < 0.001$; Figure 2) during the multichannel passive-microwave satellite era (post-1978), suggesting that sea ice and A_n are directly and/or indirectly linked. Among the numerous variables measured in the BP ice core, A_n, rather than marine originating chemical species such as Na^+, MSA, and stable water isotopes, is most strongly related to SIE. The lack of a relationship between the chemical species and SIE suggests that direct forcing is limited and that BP A_n and SIE are indirectly linked through their responses to larger-scale forcings.

Both BP A_n and Bellingshausen SIE respond to changes in the strength of the ASL (Table 1 and Figure 4), which governs the meridional flow over this region. A stronger ASL advects warm air from the north to the AP region such that BP A_n increases and Bellingshausen SIE decreases. Similarly, a weaker ASL reduces the flow of warm, northerly air to the AP region such that BP A_n decreases and Bellingshausen SIE expands. The ASL is influenced by large-scale oscillations, particularly SAM and ENSO. Cold ENSO events (i.e., La Niñas) shift the SPCZ to the southwest, deepen the ASL, and hence increase accumulation over the AP and decrease Bellingshausen SIE. Similarly, a positive SAM strengthens the circumpolar westerlies, deepens the ASL, and thereby also increases accumulation over the AP and decreases Bellingshausen SIE. Thus, the complex interactions between SAM and ENSO, and their resultant influence on the ASL, play a large role in driving the amount of BP A_n and Bellingshausen SIE. Trends over the multichannel passive-microwave satellite era (post-1978) show an increasingly positive SAM accompanied by higher BP A_n and reduced Bellingshausen SIE. However, *Goodwin et al.* [2016] demonstrated that prior to 1979, the relationship between SAM and BP A_n was quite different and exhibited multidecadal variability. Hence, we considered it important to include in our study a much longer sea ice record than the satellites provide.

The observational fast ice record from the South Orkney Islands includes annual observations of formation, breakout, and duration of sea ice near these islands in the northwestern Weddell Sea for much of the twentieth century. Comparisons suggest that BP A_n and the SOFI series are linked such that higher BP A_n is associated with earlier breakout and shorter sea ice duration (Figure 7). Also, higher BP A_n is associated with delayed formation of sea ice in the following year, suggesting that the autumn formation date is partially affected by preconditioning from the previous year (e.g., higher (lower) BP A_n is followed by later (earlier) SOFI formation). The sign of these relationships is relatively consistent for the twentieth century although the magnitude shows multidecadal variations (Figure 8). Most notably, in the 1930s and 1970s, the relationship between BP A_n and both SOFI breakout and duration weakens considerably (Figure 8). These weakened conditions appear due to atmospheric wave patterns associated with the TPI (Figure 8b) and primarily lower pressure over the Falkland Islands region. Anomalous northerly flow over the South Orkney Islands associated with lower pressure over the Falkland Islands disrupts the usual westerly flow and hence the connection between BP A_n and SOFI duration. During these periods with disrupted westerlies, however, a close relationship between BP A_n and Bellingshausen SIE is likely to be maintained as both are situated west of the Drake Passage and are in close proximity.

Given the many complicated interactions within the Earth's climate system (including in this case the nonstationary relationship between BP A_n and SAM) [*Goodwin et al.,* 2016], proxy indicators of climate variables are never perfect, and here the complications are compounded by the facts that (1) the link between BP accumulation and Bellingshausen SIE is indirect and (2) the indirect link changes with larger-scale conditions. On the positive side, the fact that the relationship between BP A_n and SOFI does not exhibit the same multidecadal sign reversals as the relationship between BP A_n and SAM [*Goodwin et al.,* 2016] suggests that when the nature of the relationship between BP A_n and SAM reverses, the relationship between Bellingshausen SIE and SAM exhibits a similar reversal. Since BP A_n and Bellingshausen SIE likely exhibit congruent responses to different large-scale forcings, it is reasonable to hypothesize a temporal consistency in their relationship. Accordingly, despite the complications, we conclude that the BP A_n record could conceivably serve as a reasonable proxy for Bellingshausen SIE prior to the satellite record. With that in mind, we also note that the

sharp increasing trend observed in BP A_n after 1970 and the accompanying reduction in Bellingshausen Sea SIE appear to be unique in the twentieth century, as similar trends in BP A_n of this magnitude do not occur earlier in the twentieth century.

Acknowledgments
The Bruce Plateau field project, laboratory analyses, and partial support for S.E.P. and E.M.T. were provided by NSF award ANT-0732655 to Ellen Mosley-Thompson as part of NSF's IPY LARISSA Project. Support for C.L.P. was provided through the NASA Earth Science Division. We thank Aaron Wilson for valuable and insightful discussions and three anonymous reviewers for their thoughtful and constructive reviews. The ice core data used in this study are archived at NOAA's National Climatic Data Center/ Paleoclimatology (https://www.ncdc.noaa.gov/cdo/f?p=519:1:0::::P1_STUDY_ID:20350). This is Byrd Polar and Climate Research Center contribution 1549.

References

Abram, N. J., R. Mulvaney, E. W. Wolff, and M. Mudelsee (2007), Ice core records as sea ice proxies: An evaluation from the Weddell Sea region of Antarctica, *J. Geophys. Res.*, *112*, D15101, doi:10.1029/2006JD008139.

Abram, N. J., E. R. Thomas, J. R. McConnell, R. Mulvaney, T. J. Bracegirdle, L. C. Sime, and A. J. Aristarain (2010), Ice core evidence for a 20th century decline of sea ice in the Bellingshausen Sea, Antarctica, *J. Geophys. Res.*, *115*, D23101, doi:10.1029/2010JD014644.

Abram, N. J., E. W. Wolff, and M. A. J. Curran (2013), A review of sea ice proxy information from polar ice cores, *Quat. Sci. Rev.*, *79*, 168–183.

Abram, N. J., R. Mulvaney, F. Vimeux, S. J. Phipps, J. Turner, and M. H. England (2014), Evolution of the Southern Annular Mode during the past millennium, *Nat. Clim. Change*, *4*, 564–569.

Ainley, D. G., C. T. Tynan, and I. Stirling (2003), Sea ice: A critical habitat for polar marine mammals and birds, in *Sea Ice: An Introduction to Its Physics, Chemistry, Biology, and Geology*, edited by D. N. Thomas and G. S. Dieckmann, pp. 240–266, Blackwell Science, Oxford.

Allan, R. J., N. Nicholls, P. D. Jones, and I. J. Butterworth (1991), A further extension of the Tahiti-Darwin SOI, early ENSO events and Darwin pressure, *J. Clim.*, *4*, 743–749.

Baines, P. G., and K. Fraedrich (1989), Topographic effects on the mean tropospheric flow patterns around Antarctica, *J. Atmos. Sci.*, *46*, 3401–3415.

Cai, W., P. H. Whetton, and D. J. Karoly (2003), The response of the Antarctic Oscillation to increasing and stabilized atmospheric CO_2, *J. Clim.*, *16*, 1525–1538.

Chen, B., S. R. Smith, and D. H. Bromwich (1996), Evolution of the tropospheric split jet over the South Pacific Ocean during the 1986–89 ENSO cycle, *Mon. Weather Rev.*, *124*, 1711–1731.

Clem, K. R., and R. L. Fogt (2013), Varying roles of ENSO and SAM on the Antarctic Peninsula climate in austral spring, *J. Geophys. Res. Atmos*, *118*, 11,481–11,492.

Clem, K. R., and R. L. Fogt (2015), South Pacific circulation changes and their connection to the tropics and regional Antarctic warming in austral spring, 1979–2012, *J. Geophys. Res. Atmos.*, *120*, 2773–2792.

Curran, M. A. J., and G. B. Jones (2000), Dimethyl sulfide in the Southern Ocean: Seasonality and flux, *J. Geophys. Res.*, *105*, 20,451–20,459, doi:10.1029/2000JD900176.

Curran, M. A. J., T. D. van Ommen, V. I. Morgan, K. L. Phillips, and A. S. Palmer (2003), Ice core evidence for Antarctic sea ice decline since the 1950s, *Science*, *302*, 1203–1206.

Dansgaard, W., and S. J. Johnsen (1969), A flow model and a time scale for the ice core from Camp Century, Greenland, *J. Glaciol.*, *53*, 215–223.

Ding, Q., E. J. Steig, D. S. Battisti, and J. M. Wallace (2012), Influence of the tropics on the Southern Annular Mode, *J. Clim.*, *25*, 6330–6348.

Dixon, D., P. A. Mayewski, S. Kaspari, K. Kreutz, G. Hamilton, K. Maasch, S. B. Sneed, and M. J. Handley (2005), A 200 year sulfate record from 16 Antarctic ice cores and associations with Southern Ocean sea ice extent, *Ann. Glaciol.*, *41*, 155–166.

Ebisuzaki, W. (1997), A method to estimate the statistical significance of a correlation when the data are serially correlated, *J. Clim.*, *10*, 2147–2153.

Eichler, T. P., and J. Gottschalck (2013), A comparison of Southern Hemisphere cyclone track climatology and interannual variability in coarse-gridded reanalysis datasets, *Adv. Meteor.*, 891260, doi:10.1155/2013/891260.

Fogt, R. L., and D. H. Bromwich (2006), Decadal variability of the ENSO teleconnection to the high-latitude South Pacific governed by coupling with the Southern Annular Mode, *J. Clim.*, *19*, 979–997.

Fogt, R. L., and A. J. Wovrosh (2015), The relative influence of tropical sea surface temperatures and radiative forcing on the Amundsen Sea Low, *J. Clim.*, *28*, 8540–8555.

Fogt, R. L., J. Perlwitz, A. J. Monaghan, D. H. Bromwich, J. M. Jones, and G. J. Marshall (2009), Historical SAM variability. Part II: Twentieth century variability and trends from reconstructions, observations, and the IPCC AR4 models, *J. Clim.*, *22*, 5346–5365.

Fogt, R. L., D. H. Bromwich, and K. M. Hines (2011), Understanding the SAM influence on the South Pacific ENSO teleconnection, *Clim. Dyn.*, *36*, 1555–1576, doi:10.1007/s00382-010-0905-0.

Fogt, R. L., A. J. Wovrosh, R. A. Langen, and I. Simmonds (2012), The characteristic variability and connection to the underlying synoptic activity of the Amundsen-Bellingshausen Sea Low, *J. Geophys. Res.*, *117*, D07111, doi:10.1029/2011JD017337.

Fyfe, J. C., G. J. Boer, and G. M. Flato (1999), The Arctic and Antarctic Oscillations and their projected changes under global warming, *Geophys. Res. Lett.*, *26*, 1601–1604, doi:10.1029/1999GL900317.

Gong, D., and S. Wang (1999), Definition of Antarctic oscillation index, *Geophys. Res. Lett.*, *26*, 459–462, doi:10.1029/1999GL900003.

Gong, T., S. B. Feldstein, and D. Luo (2010), The impact of ENSO on wave breaking and Southern Annular Mode events, *J. Atmos. Sci.*, *67*, 2854–2870, doi:10.1175/2010JAS3311.1.

Gong, T., S. B. Feldstein, and D. Luo (2013), A simple GCM study on the relationship between ENSO and the Southern Annular Mode, *J. Atmos. Sci.*, *70*, 1821–1832, doi:10.1175/JAS-D-12-0161.1.

Goodwin, B. P. (2013), Recent environmental changes on the Antarctic Peninsula as recorded in an ice core from the Bruce Plateau, PhD dissertation, Dep. of Geogr., Atmos. Sci. Program., The Ohio State Univ., Columbus.

Goodwin, B. P., E. Mosley-Thompson, A. B. Wilson, S. E. Porter, and M. R. Sierra-Hernandez (2016), Accumulation variability in the Antarctic Peninsula: The role of large-scale atmospheric oscillations and their interactions, *J. Clim.*, *29*, 2579–2596.

Holland, P. R., and R. Kwok (2012), Wind-driven trends in Antarctic sea-ice drift, *Nat. Geosci.*, *5*, 872–875.

Hosking, J. S., A. Orr, T. J. Bracegirdle, and J. Turner (2016), Future circulation changes off West Antarctica: Sensitivity of the Amundsen Sea Low to projected anthropogenic forcing, *Geophys. Res. Lett.*, *43*, 367–376, doi:10.1002/2015GL067143.

Jones, P. D., M. J. Salinger, and A. B. Mullan (1999), Extratropical circulation indices in the Southern Hemisphere based on station data, *Int. J. Climatol.*, *19*, 1301–1317.

Kalnay, E., et al. (1996), The NCEP/NCAR 40-year reanalysis project, *Bull. Am. Meteorol. Soc.*, *77*, 437–471.

Können, G. P., P. D. Jones, M. H. Kaltofen, and R. J. Allan (1998), Pre-1866 extensions of the Southern Oscillation Index using early Indonesian and Tahitian meteorological readings, *J. Clim.*, *11*, 2325–2339.

Kushner, P. J., I. M. Held, and T. L. Delworth (2001), Southern Hemisphere atmospheric circulation response to global warming, *J. Clim.*, *14*, 2238–2249.

Küttel, M., E. J. Steig, Q. Ding, A. J. Monaghan, and D. S. Battisti (2012), Seasonal climate information preserved in West Antarctic ice core water isotopes: Relationships to temperature, large-scale circulation, and sea ice, *Clim. Dyn.*, *39*, 1841–1857.
Kvamstø, N. G., P. Skeie, and D. B. Stephenson (2004), Impact of Labrador sea-ice extent on the North Atlantic Oscillation, *Int. J. Climatol.*, *24*, 603–612.
Kwok, R., and J. C. Comiso (2002), Southern Ocean climate and sea ice anomalies associated with the Southern Oscillation, *J. Clim.*, *15*, 487–501.
Lachlan-Cope, T. A., and W. M. Connolley (2006), Teleconnections between the tropical Pacific and the Amundsen-Bellingshausen Sea: Role of the El-Niño/Southern Oscillation, *J. Geophys. Res.*, *111*, D23101, doi:10.1029/2005JD006386.
Lachlan-Cope, T. A., W. M. Connolley, and J. Turner (2001), The role of the non-axisymmetric Antarctic orography in forcing the observed pattern of variability of the Antarctic climate, *Geophys. Res. Lett.*, *28*, 4111–4114, doi:10.1029/2001GL013465.
Lefebvre, W., H. Goosse, R. Timmermann, and T. Fichefet (2004), Influence of the Southern Annular Mode on the sea ice-ocean system, *J. Geophys. Res.*, *109*, C09005, doi:10.1029/2004JC002403.
L'Heureux, M. L., and D. W. J. Thompson (2006), Observed relationships between the El Niño/Southern Oscillation and the extratropical zonal-mean circulation, *J. Clim.*, *19*, 276–287.
MacGregor, J. A., K. Matsuoka, E. D. Waddington, D. P. Winebrenner, and F. Pattyn (2012), Spatial variation of englacial radar attenuation: Modeling approach and application to the Vostok flowline, *J. Geophys. Res.*, *117*, F03022, doi:10.1029/2011JF002327.
Marshall, G. J. (2003), Trends in the southern annular mode from observations and reanalyses, *J. Clim.*, *16*, 4134–4143.
Marshall, G. J., A. Orr, and J. Turner (2013), A predominant reversal in the relationship between the SAM and East Antarctic temperatures during the twenty-first century, *J. Clim.*, *26*, 5196–5204.
Miles, G. M., G. J. Marshall, J. R. McConnell, and A. J. Aristarain (2008), Recent accumulation variability and change on the Antarctic Peninsula from the ERA-40 reanalysis, *Int. J. Climatol.*, *28*, 1409–1422, doi:10.1002/joc.1642.
Murphy, E. J., A. Clarke, C. Symon, and J. Priddle (1995), Temporal variation in Antarctic sea-ice: Analysis of a long term fast-ice record from the South Orkney Islands, *Deep Sea Res., Part I*, *42*, 1045–1062.
Murphy, E. J., A. Clarke, N. J. Abram, and J. Turner (2014), Variability of sea-ice in the northern Weddell Sea during the 20th century, *J. Geophys. Res. Oceans*, *119*, 4549–4572.
Nye, J. F. (1963), Correction factor for accumulation measured by thickness of annual layers in an ice sheet, *J. Glaciol.*, *4*, 785–788.
Parkinson, C. L. (2004), Southern Ocean sea ice and its wider linkages: Insights revealed from models and observations, *Antarct. Sci.*, *16*(4), 387–400, doi:10.1017/S0954102004002214.
Parkinson, C. L., and D. J. Cavalieri (2012), Antarctic sea ice variability and trends, 1979–2010, *Cryosphere*, *6*, 871–880, doi:10.5194/tc-6-871-2012.
Pasteur, E. C., and R. Mulvaney (2000), Migration of methane sulfonate in Antarctic firn and ice, *J. Geophys. Res.*, *105*, 11,525–11,534, doi:10.1029/2000JD900006.
Pittock, A. B. (1980), Patterns of climatic variation in Argentina and Chile—I: Precipitation, 1931–60, *Mon. Weather Rev.*, *108*, 1347–1361.
Pittock, A. B. (1984), On the reality, stability, and usefulness of Southern Hemisphere teleconnections, *Aust. Meteor. Mag.*, *32*, 75–82.
Post, E., U. S. Bhatt, C. M. Bitz, J. F. Brodie, T. L. Fulton, M. Hebblewhite, J. Kerby, S. J. Kutz, I. Stirling, and D. A. Walker (2013), Ecological consequences of sea-ice decline, *Science*, *341*(6145), 519–524.
Pourchet, M., F. Pinglot, and C. Lorius (1983), Some meteorological applications of radioactive fallout measurements in Antarctic snows, *J. Geophys. Res.*, *88*, 6013–6020, doi:10.1029/JC088iC10p06013.
Raphael, M. N., G. J. Marshall, J. Turner, R. L. Fogt, D. Schneider, D. A. Dixon, J. S. Hosking, J. M. Jones, and W. R. Hobbs (2016), The Amundsen Sea Low: Variability, change, and impact on Antarctic climate, *Bull. Am. Meteorol. Soc.*, *97*, 111–121.
Ropelewski, C. F., and P. D. Jones (1987), An extension of the Tahiti-Darwin Southern Oscillation Index, *Mon. Weather Rev.*, *115*, 2161–2165.
Röthlisberger, R., X. Crosta, N. J. Abram, L. Armand, and E. W. Wolff (2010), Potential and limitations of marine and ice core sea ice proxies: An example from the Indian Ocean sector, *Quat. Sci. Rev.*, *29*, 296–302.
Scambos, T. A., J. A. Bohlander, C. A. Shuman, and P. Skvarca (2004), Glacier acceleration and thinning after ice shelf collapse in the Larsen B embayment, Antarctica, *J. Geophys. Res.*, *31*, L18402, doi:10.1029/2004GL020670.
Shindell, D. T., and G. A. Schmidt (2004), Southern Hemisphere climate response to ozone changes and greenhouse gas increases, *Geophys. Res. Lett.*, *31*, L18209, doi:10.1029/2004GL020724.
Silvestri, G., and C. Vera (2009), Nonstationary impacts of the Southern Annular Mode on Southern Hemisphere climate, *J. Clim.*, *22*, 6142–6148.
Stammerjohn, S. E., D. G. Martinson, R. C. Smith, X. Yuan, and D. Rind (2008), Trends in Antarctic annual sea ice retreat and advance and their relation to El-Niño-Southern Oscillation and Southern Annular Mode variability, *J. Geophys. Res.*, *113*, C03S90, doi:10.1029/2007JC004269.
Thomas, E. R., and N. J. Abram (2016), Ice core reconstruction of sea ice change in the Amundsen-Ross-Seas since 1702 A.D, *Geophys. Res. Lett.*, *43*, 5309–5317, doi:10.1002/2016GL068130.
Thomas, E. R., G. J. Marshall, and J. R. McConnell (2008), A doubling in snow accumulation in the western Antarctic Peninsula since 1850, *Geophys. Res. Lett.*, *35*, L01706, doi:10.1029/2007GL032529.
Thomas, E. R., T. J. Bracegirdle, J. Turner, and E. W. Wolff (2013), A 308 year record of climate variability in West Antarctica, *Geophys. Res. Lett.*, *40*, 5492–5496, doi:10.1002/2013GL057782.
Thomas, E. R., J. S. Hosking, R. R. Tuckwell, R. A. Warren, and E. C. Ludlow (2015), Twentieth century increase in snowfall in coastal West Antarctica, *Geophys. Res. Lett.*, *42*, 9387–9393, doi:10.1002/2015GL065750.
Thompson, D. W. J., and S. Solomon (2002), Interpretation of recent Southern Hemisphere climate change, *Science*, *296*, 895–899.
Thompson, D. W. J., and J. M. Wallace (2000), Annular modes in the extratropical circulation. Part I: Month-to-month variability, *J. Clim.*, *13*, 1000–1016.
Thompson, D. W. J., S. Solomon, P. J. Kushner, M. H. England, K. M. Grise, and D. J. Karoly (2011), Signatures of the Antarctic ozone hole in Southern Hemisphere surface climate change, *Nat. Geosci.*, *4*, 741–749.
Thompson, L. G., D. A. Peel, E. Mosley-Thompson, R. Mulvaney, J. Dai, P.-N. Lin, M. E. Davis, and C. F. Raymond (1994), Climate since AD 1510 on Dyer Plateau, Antarctic Peninsula: Evidence for recent climatic change, *Ann. Glaciol.*, *20*, 420–426.
Turner, J. (2004), The El-Niño-Southern Oscillation and Antarctica, *Int. J. Climatol.*, *24*, 1–31.
Turner, J., S. R. Colwell, G. J. Marshall, T. A. Lachlan-Cope, A. M. Carleton, P. D. Jones, V. Lagun, P. A. Reid, and S. Iagovkina (2005), Antarctic climate change during the last 50 years, *Int. J. Climatol.*, *25*, 279–294.
Turner, J., T. Phillips, J. S. Hosking, G. J. Marshall, and A. Orr (2013), The Amundsen Sea Low, *Int. J. Climatol.*, *33*, 1818–1829.

Vincent, D. G. (1994), The South Pacific Convergence Zone (SPCZ): A review, *Mon. Weather Rev.*, *122*, 1949–1970.
Wolff, E. W., et al. (2006), Southern Ocean sea-ice extent, productivity and iron flux over the past eight glacial cycles, *Nature*, *440*, 491–496.
Zagorodnov, V., O. Nagornov, T. A. Scambos, A. Muto, E. Mosley-Thompson, E. C. Pettit, and S. Tyuflin (2012), Borehole temperatures reveal details of 20th century warming at Bruce Plateau, Antarctic Peninsula, *Cryosphere*, *6*, 675–686.
Zheng, F., J. Li, R. T. Clark, and H. C. Nnamchi (2013), Simulation and projection of the Southern Hemisphere Annular Mode in CMIP5 models, *J. Clim.*, *26*, 9860–9879.